



Flexible Zirconium Metal–Organic Frameworks as Bioinspired Switchable Catalysts

Shuai Yuan⁺, Lanfang Zou⁺, Haixia Li, Ying-Pin Chen, Junsheng Qin, Qiang Zhang, Weigang Lu,^{*} Michael B. Hall,^{*} and Hong-Cai Zhou^{*}

Abstract: Flexible metal–organic frameworks (MOFs) are highly desirable in host–guest chemistry owing to their almost unlimited structural/functional diversities and stimuli-responsive pore architectures. Herein, we designed a flexible Zr-MOF system, namely PCN-700 series, for the realization of switchable catalysis in cycloaddition reactions of CO₂ with epoxides. Their breathing behaviors were studied by successive single-crystal X-ray diffraction analyses. The breathing amplitudes of the PCN-700 series were modulated through pre-functionalization of organic linkers and post-synthetic linker installation. Experiments and molecular simulations confirm that the catalytic activities of the PCN-700 series can be switched on and off upon reversible structural transformation, which is reminiscent of sophisticated biological systems such as allosteric enzymes.

In nature, enzyme activity is often modulated through feedback loops and a variety of trigger-induced effects. Inspired by nature, chemists have been developing catalysts whose activity can be controlled by external stimuli.^[1] Such systems are capable of alternating the environment of their active centers, which in turn regulates the reaction rate and selectivity, functioning as allosteric catalysts.^[2] Flexible metal–organic frameworks (MOFs) are suitable platforms for the development of artificial switchable catalysts in consideration of their inherent cavities and dynamic behaviors.^[3] They are capable of responding to various chemical and physical stimuli, such as light, pressure, temperature, or guest molecules.^[4] A prominent example is the well-established “breathing behavior”, in which the framework experiences a reversible unit-cell dimensional change as a result of host–guest interactions.^[5] Different from other porous materials, such as zeolites and activated carbons, flexible MOFs respond to the stimuli with retention of high regularity, which allows

for structure characterization by means of crystallography, therefore maximizing the understanding of correlation between applied stimuli and ensuing properties.^[6] Additionally, the inherent cavities and dynamic behaviors of flexible MOFs are reminiscent of sophisticated biological systems, such as regulatory enzymes, in which stimuli induce conformational changes and variations of catalytic activities.

High stability and dynamic pore architecture are indispensable in switchable MOF catalysts. The Zr₆ cluster, in this regard, is a promising building unit for the construction of switchable MOF catalysts. The dihedral angles between the Zr₆ clusters and carboxylate linkers vary from 0 to 14.5° in various Zr-MOFs, suggesting extensive flexibility in the Zr-carboxylate junction.^[7] In addition, the chemical inertness of Zr–O bonds make the Zr-MOFs robust platforms for a variety of catalytic applications.^[8] Although Zr-MOFs are one of the research focuses in recent years, the reported Zr-MOFs usually show limited breathing amplitude that mainly resulted from linker flexibility.^[9] This promotes us to develop flexible Zr-MOFs for the realization of switchable catalysis.

A Zr-MOF with flexible **bcu** topology, namely PCN-700-Me₂, was selected as a prototype MOF.^[12b] PCN-700-Me₂ crystallizes in the tetragonal space group *P4₂/mmc*. Each Zr₆ cluster is coordinated to eight Me₂-BPDC linkers (Me₂-BPDC = 2,2'-dimethylbiphenyl-4,4'-dicarboxylate) and eight terminal -OH/H₂O groups. The overall framework can be simplified into a flexible **bcu** net, which is expected to shrink along the *c*-axis while expanding within the *ab*-plane (Figure S4 in the Supporting Information). Breathing behaviors of MOFs are usually triggered by the removal or introduction of guest molecules. Bearing this in mind, we carried out successive single-crystal X-ray diffraction (SC-XRD) analyses on PCN-700-Me₂ during desolvation to generate “snapshots” of the breathing process. Crystallographic data clearly shows that PCN-700-Me₂ exhibits a “scissor-jack-like” behavior, shrinking along *c*-direction by tweaking the metal–linker angle (Figure 1 a). A significant decrease in the length of *c*-axis (from 14.92 Å to 11.24 Å) and a slight increase in the length of *ab*-axis (from 24.35 Å to 24.84 Å) were observed upon guest removal. The flexible Zr-carboxylate connection, acting as a hinge, is primarily responsible for the breathing behavior. As shown in Figure 1 e,f, PCN-700-Me₂ undergoes a large conformational change that is associated with the bending of Zr–O–C angle (from 133° to 130°) and, more intuitively, the varying of dihedral angle between the equatorial plane of O–Zr–O and the plane of carboxylate (from 10° to 32°). The bending of Zr–carboxylate bond affords a closer packing along *c*-direction, which gives rise to a shrinkage of the *c*-axis. A closer investigation indicates

[*] S. Yuan,^[†] L. Zou,^[†] Dr. H. Li, Y.-P. Chen, Dr. J. Qin, Dr. Q. Zhang, Prof. Dr. M. B. Hall, Prof. Dr. H.-C. Zhou
Department of Chemistry
Texas A&M University
College Station, TX 77843 (USA)
E-mail: hall@science.tamu.edu
zhou@chem.tamu.edu

Dr. W. Lu
Department of Chemistry, Blinn College
Bryan, TX 77805 (USA)
E-mail: weiganglu@yahoo.com

[†] These authors contributed equally to this work.

Supporting information and the ORCID identification number(s) for the author(s) of this article can be found under <http://dx.doi.org/10.1002/anie.201604313>.

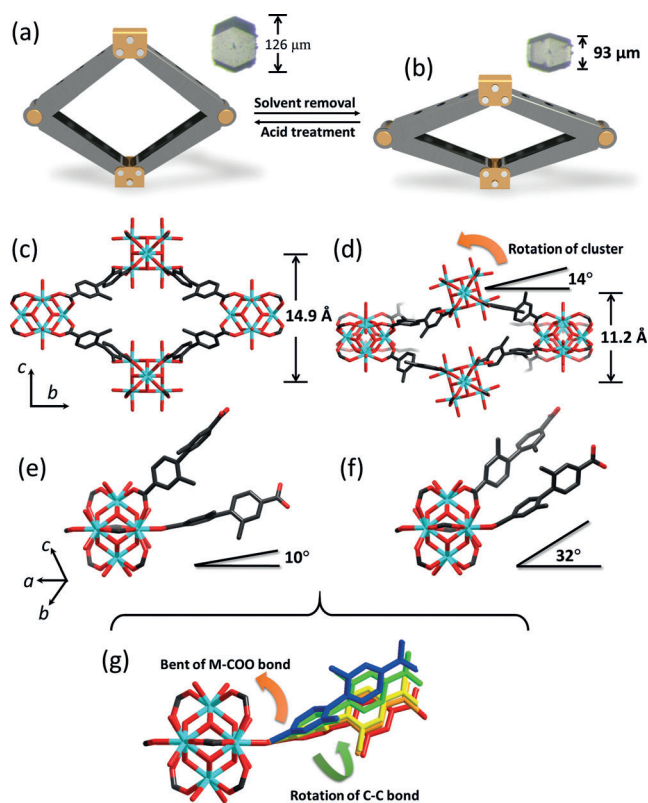


Figure 1. a),b) Schematic representations of PCN-700-Me₂ before and after desolvation. Insets: photos of microscope images of the respective single crystals. c),d) Structures of PCN-700-Me₂ before and after desolvation. e),f) Linker conformation before and after desolvation. g) An overlap of structural conformations during desolvation.

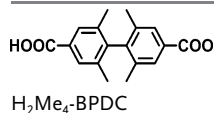
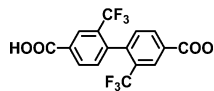
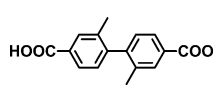
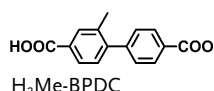
that the breathing motion of PCN-700-Me₂ is a collective result. Along with the bending of Zr-carboxylate bond, we also observed a rotation of the C-C bond between two phenyl rings, which alleviates the steric hindrance within the structure by arranging the two methyl groups on adjacent linkers as far apart as possible. As a collateral effect of the rotation of C-C bond, Zr₆ clusters tilt about 14° (Figure 1 d). An overlap of different conformations during desolvation (Figure 1 g) underlines the fact that the bending of Zr-carboxylate junction and the conformational change of the organic linker together account for the breathing behavior of PCN-700-Me₂.

It should be noted that the axial breathing amplitude of PCN-700-Me₂ is much larger than the volumetric breathing amplitude. The nearly uniaxial breathing behavior can be directly observed on a real crystal under optical microscope. One particular PCN-700-Me₂ crystal was measured with a length of 126 μm along *c*-axis, which shrank to 93 μm (Figure 1 a,b) upon desolvation (*c*-direction is determined by Apex 2, Figure S1). These values match very well with unit-cell parameters determined by SC-XRD. Such high elasticity in macroscopic single crystals is rarely observed to our knowledge.^[10]

The SC-XRD investigation of the breathing mechanism manifests the structure-property correlations, which further enable us to judiciously modulate the flexibility of the PCN-

700 system. Since PCN-700-Me₂ undergoes unit-cell dimensional contraction along *c*-axis, which involves a rotation of the C-C bond between phenyl rings, we speculate that the framework flexibility can be tuned by changing substituents on phenyl rings of the linker. To tune the breathing amplitude, linkers with different substituents were selected, namely H₂Me₄-BPDC (2,2',6,6'-tetramethylbiphenyl-4,4'-dicarboxylic acid), H₂(CF₃)₂-BPDC (2,2'-bis(trifluoromethyl)biphenyl-4,4'-dicarboxylic acid), and H₂Me-BPDC (2-methylbiphenyl-4,4'-dicarboxylic acid; Table 1). As expected, H₂Me₄-BPDC and H₂(CF₃)₂-BPDC give rise to MOFs with increased

Table 1: Tuning the breathing amplitude by linker modification.

Linker	Topology	DMF <i>c</i> [Å]	Dry <i>c</i> [Å]	Δ <i>c</i> [%]
	bcu	15.4	14.1	9.22
H ₂ Me ₄ -BPDC				
	bcu	15.0	12.1	24.0
H ₂ (CF ₃) ₂ -BPDC				
	bcu	14.9	11.2	33.0
H ₂ Me ₂ -BPDC				
	fcu	26.7	26.7	0
H ₂ Me-BPDC				

structural rigidity because of the elevated steric hindrance. Among this series, PCN-700-Me₄ exhibits the highest degree of rigidity while only small changes of *c*-axis length (15.4 Å to 14.1 Å) and unit cell volume (9008 Å³ to 8170 Å³) were observed upon desolvation (Table 1 and Table S3). Intuitively, linkers with less-bulky substituents tend to form more flexible MOF structures, as demonstrated in MIL-53 and MIL-88 systems.^[11] However, this is not the case in PCN-700 system. The substituents on the phenyl rings are required to be bulky enough to induce two off-plane carboxylate groups. As far as steric hindrance is concerned, H₂Me-BPDC is expected to generate an even more flexible MOF than PCN-700-Me₂. However, only an **fcu** net (UiO-67 analogue) was obtained by using H₂Me-BPDC. PCN-700-Me₂ is by far, the most flexible MOF that we obtained with the **bcu** topology.

The breathing amplitude of PCN-700-Me₂ can also be manipulated through linker installation. It has been proved that dicarboxylate linkers with different lengths can be installed between Zr₆ clusters (Scheme S5).^[12] Four linear linkers with different lengths, namely FA (fumarate), BDC (1,4-benzenedicarboxylate), NDC (2,6-naphthalene dicarboxylate), and BPDC (4,4'-biphenyldicarboxylate), were selected and installed in PCN-700 respectively. To carry out linker installation, PCN-700-Me₂ crystals were soaked in a DMF

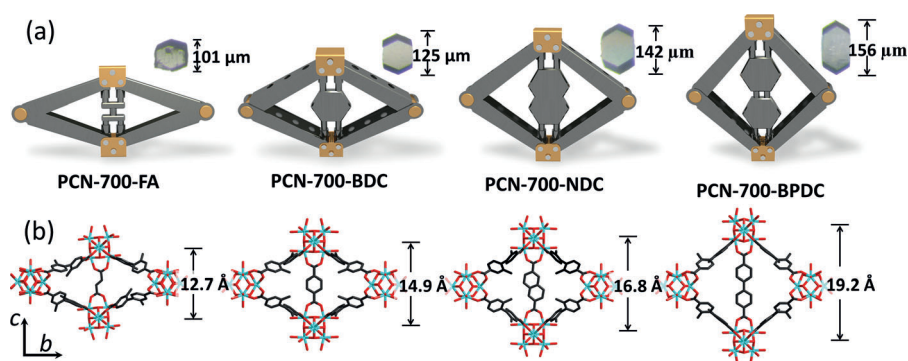


Figure 2. a) Representations and b) structures of PCN-700-Me₂ with different linkers installed. Insets: photos of the microscope view of the corresponding single crystal.

solution of linear linker at 75 °C for 24 h. The subsequently installed linkers are unambiguously observed by SC-XRD. As illustrated in Figure 2a, the subsequently installed linkers support the MOF structure just like the “jack screws” support the scissor jack. The channel size along the *a*-axis directly correlates to the linker length as shown by SC-XRD (Figure 2b) and reinforced by PXRD patterns and N₂ isotherms (Figure S5–S32). It is worth pointing out that the linker installation can induce a much larger unit cell dimension change (62% contraction along *c*-axis) than the removal of solvent (32% contraction along *c*-axis), indicating that a larger breathing amplitude can be achieved by stronger guest–host interactions, such as coordination bonds (see Supporting Information for details).

The inherent cavities and dynamic behaviors of flexible MOFs allow the cavity environment to be tuned by external stimuli, which could in turn influence the catalytic activity of the encapsulated catalyst (Figure S38). Nevertheless, flexible MOFs for switchable catalysis have not been widely explored. This could be ascribed to the fact that the close-conformation of flexible MOFs can be opened up by solvent molecules under common catalytic conditions. In contrast to most flexible MOFs, PCN-700-Me₂ shows a very limited dependence on the solvents (Table S2). The desolvated PCN-700-Me₂ maintains its shrunken structure in DMF at room temperature and is only reversed by treating with trifluoroacetic acid/DMF solution. These observations suggest that PCN-700-Me₂ solid can be considered as “rigid” under common catalytic reaction conditions. The closed conformation and opened conformation are expected to show different catalytic activity in the same solvent.

As a proof of concept, the cycloaddition reaction of CO₂ with epoxides was selected to evaluate the Lewis-acid catalytic activity of PCN-700-Me₂.^[13] The performances of as-synthesized PCN-700-Me₂ (denoted as PCN-700-o, stands for open conformation) and desolvated PCN-700-Me₂ (denoted as PCN-700-c, stands for closed conformation) samples were evaluated with different epoxides at 50 °C under 1 atm CO₂ pressure and solvent-free condition. As shown in Table 2, the desolvated sample, PCN-700-c, shows prominently decreased performance. Yet, the catalytic activity of PCN-700-c can be restored by trifluoroacetic acid/DMF treatment which expands the shrunken structure to the

original configuration. The catalytic activity of PCN-700-Me₂ was turned on and off for four times, demonstrating a successful reversible control of the catalytic activity towards CO₂ fixation reaction (Figure S42).

To elucidate the mechanism of the switchable catalytic activity, control experiments were further conducted. The difference in catalytic activity of PCN-700-o and PCN-700-c could be possibly attributed to 1) different diffusion rates of substrate and 2) different Lewis acid sites. To eliminate the influence of substrate diffusion, V_{\max} was mea-

Table 2: Catalytic reaction of CO₂ and epoxides.

Entry	R	Catalyst	Conversion [%] ^[a]	TON ^[b]	TOF [h ⁻¹] ^[c]
1	Me	–	15.1	–	–
2	Me	ZrCl ₄	67.9	131.8	13.2
3	Me	700-o	93.2	244.0	24.4
4	Me	700-c	29.1	76.2	7.6
5	Ph	700-o	83.3	218.0	21.8
6	Ph	700-c	37.0	96.9	9.7
7	Et	700-o	91.7	240.0	24.0
8	Et	700-c	27.5	72.0	7.2
9	CH ₂ Cl	700-o	92.3	241.6	24.2
10	CH ₂ Cl	700-c	30.2	79.0	7.9

[a] Conversion calculated from the ¹H NMR spectra. [b] Turnover number (product (mmol)/metal (mmol)). [c] Turnover frequency (product (mmol)/metal (mmol)/time (h)).

sured which represents the maximum rate achieved by catalysts at saturating substrate concentrations. V_{\max} of PCN-700-o and PCN-700-c was calculated to be 42.9 and 6.95 mmol min⁻¹ respectively, showing a clear difference in maximum reaction velocity. Usually, V_{\max} depends on the efficiency and concentration of active sites, which is believed to be the -OH⁻/H₂O groups on the Zr₆ clusters.^[13] To prove this, control experiments were carried out under the same condition using UiO-67 as a Lewis acid, which has no accessible -OH⁻/H₂O groups on the clusters. The V_{\max} (UiO-67) was tested to be 4.54 mmol min⁻¹, which is about 10 times smaller than that of V_{\max} (PCN-700-o), indicating the prominent influence of -OH⁻/H₂O groups. In PCN-700 structure, there are two pairs of symmetrically independent -OH⁻/H₂O groups on one Zr₆ cluster along *c*-direction and *b*-direction, respectively. The -OH⁻/H₂O groups along *c*-direction and *b*-direction in PCN-700-o are both accessible by substrates (Figure 3a), whereas -OH⁻/H₂O groups in PCN-700-c are only accessible from the *b*-direction, because of the close

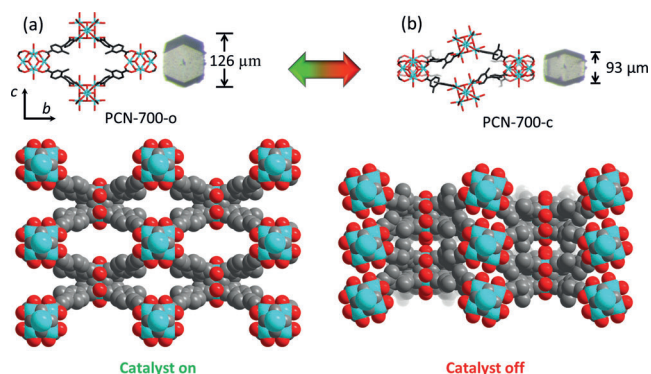


Figure 3. Structure of PCN-700-o (a) and PCN-700-c (b) showing the accessibility of the active $\text{-OH}^-/\text{H}_2\text{O}$ centers (which are shown in red).

packing of ligand and clusters along the c -direction, leaving no room for substrates (Figure 3b).

The halved active site in PCN-700-c is expected to reduce the V_{max} by half. However, the experimental data suggested that the V_{max} (PCN-700-c) is actually reduced by 84% compared to that of V_{max} (PCN-700-o). We propose that the $\text{-OH}^-/\text{H}_2\text{O}$ groups along c -direction are more active than those along b -direction, thus burying the $\text{-OH}^-/\text{H}_2\text{O}$ groups along c -direction caused a dramatic decrease in catalytic activity for PCN-700-c. Indeed, we observed that the $\text{-OH}^-/\text{H}_2\text{O}$ groups along c -direction selectively deprotonate to react with basic metal hydroxides, whereas the $\text{-OH}^-/\text{H}_2\text{O}$ groups along the b -direction tend to act as bases to react with molybdic acid (Figure S46).^[14] To further support our hypothesis, we used density functional theory (DFT) to calculate the relative acidities of Zr_6 models of PCN-700-o and PCN-700-c (see Supporting Information, Section S9). The calculated $\Delta\text{p}K_{\text{a}}$ value for the PCN-700-o- Zr_6 model (the $\text{p}K_{\text{a}}$ of $\text{-OH}^-/\text{H}_2\text{O}$ along the b -direction minus the one along the c -direction) is 0.56. Similarly, this $\Delta\text{p}K_{\text{a}}$ value for the PCN-700-c- Zr_6 model is 2.82. The different acidity in the two directions can be tentatively attributed to the unequal electron distribution resulting from the asymmetric organic linkers. Consistent with this explanation, the asymmetric character is more notable in PCN-700-c than that in PCN-700-o, which explains the larger $\Delta\text{p}K_{\text{a}}$ value of PCN-700-c- Zr_6 than that of PCN-700-o- Zr_6 . Thus, the remarkable decrease of acidity along the b -direction, as well as the only availability of the b -direction for catalysis in PCN-700-c, results in a much lower catalytic activity of PCN-700-c than that of PCN-700-o. In short, upon removal of solvent, PCN-700- Me_2 experiences a dramatic shrinkage along c -axis which changes the cavity environment and catalytic activity.

In summary, we have conducted a comprehensive study on flexible Zr-MOFs as switchable catalysts. Single-crystal X-ray diffraction was employed to study the mechanism of the structural transformation. Organic linkers with different functional groups were utilized to rationally adjust the framework flexibility. A linker installation strategy was exploited to magnify the breathing amplitude. Furthermore, the activity of PCN-700- Me_2 as a Lewis acid catalyst can be turned on and off by structural breathing, making it a switchable catalyst. We believe that the concept of switchable

catalysis within flexible MOF systems will not only lead to a new generation of catalysts, but also open up a field of study intersecting with both crystalline porous materials and switchable catalysts.

Acknowledgements

The gas adsorption-desorption studies of this research was supported by the Center for Gas Separations Relevant to Clean Energy Technologies, an Energy Frontier Research Center funded by the U.S. Department of Energy, Office of Science, Office of Basic Energy Sciences under Award Number DE-SC0001015. Structural analyses were supported as part of the Hydrogen and Fuel Cell Program under Award Number DE-EE-0007049. H. Li and M. B. Hall acknowledge the National Science Foundation (CHE-1300787) and the Welch Foundation (A-0648) for financial support and the Texas A&M Supercomputing Facility for providing computing resources. We also acknowledge the financial support of the U.S. Department of Energy Office of Fossil Energy, National Energy Technology Laboratory (DE-FE0026472). S.Y. also acknowledges the Texas A&M Energy Institute Graduate Fellowship funded by ConocoPhillips and Dow Chemical Graduate Fellowship. We thank Mr. Mathieu Bosch for his proofreading and feedback.

Keywords: bioinspired catalysts · epoxides · flexible MOFs · pore opening · switchable catalysts

- [1] a) L. Kovbasyuk, R. Krämer, *Chem. Rev.* **2004**, *104*, 3161; b) V. Blanco, D. A. Leigh, V. Marcos, *Chem. Soc. Rev.* **2015**, *44*, 5341.
- [2] a) H. J. Yoon, J. Kuwabara, J.-H. Kim, C. A. Mirkin, *Science* **2010**, *330*, 66; b) X. Tian, C. Cassani, Y. Liu, A. Moran, A. Urakawa, P. Galzerano, E. Arceo, P. Melchiorre, *J. Am. Chem. Soc.* **2011**, *133*, 17934; c) S. Arseniyadis, A. Valleix, A. Wagner, C. Mioskowski, *Angew. Chem. Int. Ed.* **2004**, *43*, 3314; *Angew. Chem.* **2004**, *116*, 3376.
- [3] a) S. Horike, S. Shimomura, S. Kitagawa, *Nat. Chem.* **2009**, *1*, 695; b) L. Chen, J. P. Mowat, D. Fairen-Jimenez, C. A. Morrison, S. P. Thompson, P. A. Wright, T. Duren, *J. Am. Chem. Soc.* **2013**, *135*, 15763; c) L. Sarkisov, R. L. Martin, M. Haranczyk, B. Smit, *J. Am. Chem. Soc.* **2014**, *136*, 2228; d) A. Schneemann, V. Bon, I. Schwedler, I. Senkowska, S. Kaskel, R. A. Fischer, *Chem. Soc. Rev.* **2014**, *43*, 6062; e) C. Serre, C. Mellot-Draznieks, S. Surlblé, N. Audebrand, Y. Filinchuk, G. Férey, *Science* **2007**, *315*, 1828; f) K. Uemura, R. Matsuda, S. Kitagawa, *J. Solid State Chem.* **2005**, *178*, 2420.
- [4] a) F.-X. Coudert, *Chem. Mater.* **2015**, *27*, 1905; b) D. Liu, T.-F. Liu, Y.-P. Chen, L. Zou, D. Feng, K. Wang, Q. Zhang, S. Yuan, C. Zhong, H.-C. Zhou, *J. Am. Chem. Soc.* **2015**, *137*, 7740; c) N. Yanai, T. Uemura, M. Inoue, R. Matsuda, T. Fukushima, M. Tsujimoto, S. Isoda, S. Kitagawa, *J. Am. Chem. Soc.* **2012**, *134*, 4501.
- [5] a) C. Serre, F. Millange, C. Thouvenot, M. Noguès, G. Marsolier, D. Louër, G. Férey, *J. Am. Chem. Soc.* **2002**, *124*, 13519; b) P. L. Llewellyn, S. Bourrelly, C. Serre, Y. Filinchuk, G. Férey, *Angew. Chem. Int. Ed.* **2006**, *45*, 7751; *Angew. Chem.* **2006**, *118*, 7915; c) H. Sato, et al., *Science* **2014**, *343*, 167; d) J. A. Mason, et al., *Nature* **2015**, *527*, 357.

- [6] a) T. M. McDonald, et. al., *Nature* **2015**, *519*, 303; b) W. M. Bloch, A. Burgun, C. J. Coghlan, R. Lee, M. L. Coote, C. J. Doonan, C. J. Sumby, *Nat. Chem.* **2014**, *6*, 906; c) Y.-S. Wei, K.-J. Chen, P.-Q. Liao, B.-Y. Zhu, R.-B. Lin, H.-L. Zhou, B.-Y. Wang, W. Xue, J.-P. Zhang, X.-M. Chen, *Chem. Sci.* **2013**, *4*, 1539.
- [7] a) J. H. Cavka, S. Jakobsen, U. Olsbye, N. Guillou, C. Lamberti, S. Bordiga, K. P. Lillerud, *J. Am. Chem. Soc.* **2008**, *130*, 13850; b) H. Furukawa, F. Gándara, Y.-B. Zhang, J. Jiang, W. L. Queen, M. R. Hudson, O. M. Yaghi, *J. Am. Chem. Soc.* **2014**, *136*, 4369.
- [8] T. Sawano, N. C. Thacker, Z. Lin, A. R. McIsaac, W. Lin, *J. Am. Chem. Soc.* **2015**, *137*, 12241.
- [9] a) P. Deria, D. A. Gómez-Gualdrón, W. Bury, H. T. Schaef, T. C. Wang, P. K. Thallapally, A. A. Sarjeant, R. Q. Snurr, J. T. Hupp, O. K. Farha, *J. Am. Chem. Soc.* **2015**, *137*, 13183; b) Q. Zhang, J. Su, D. Feng, Z. Wei, X. Zou, H.-C. Zhou, *J. Am. Chem. Soc.* **2015**, *137*, 10064.
- [10] G. Simmons, Single-crystal elastic constants and calculated aggregate properties, **1965**.
- [11] a) P. Horcajada, F. Salles, S. Wuttke, T. Devic, D. Heurtaux, G. Maurin, A. Vimont, M. Daturi, O. David, E. Magnier, N. Stock, Y. Filinchuk, D. Popov, C. Riekkel, G. Ferey, C. Serre, *J. Am. Chem. Soc.* **2011**, *133*, 17839; b) T. Lescouet, E. Kockrick, G. Bergeret, M. Pera-Titus, S. Aguado, D. Farrusseng, *J. Mater. Chem.* **2012**, *22*, 10287.
- [12] a) P. Deria, J. E. Mondloch, E. Tylianakis, P. Ghosh, W. Bury, R. Q. Snurr, J. T. Hupp, O. K. Farha, *J. Am. Chem. Soc.* **2013**, *135*, 16801; b) S. Yuan, W. Lu, Y.-P. Chen, Q. Zhang, T.-F. Liu, D. Feng, X. Wang, J. Qin, H.-C. Zhou, *J. Am. Chem. Soc.* **2015**, *137*, 3177; c) J. Jiang, F. Gándara, Y.-B. Zhang, K. Na, O. M. Yaghi, W. G. Klemperer, *J. Am. Chem. Soc.* **2014**, *136*, 12844; d) S. Yuan, Y.-P. Chen, J. Qin, W. Lu, L. Zou, Q. Zhang, X. Wang, X. Sun, H.-C. Zhou, *J. Am. Chem. Soc.* **2016**, DOI: 10.1021/jacs.6b04501.
- [13] M. H. Beyzavi, R. C. Klet, S. Tussupbayev, J. Borycz, N. A. Vermeulen, C. J. Cramer, J. F. Stoddart, J. T. Hupp, O. K. Farha, *J. Am. Chem. Soc.* **2014**, *136*, 15861.
- [14] S. Yuan, Y.-P. Chen, J. Qin, W. Lu, X. Wang, Q. Zhang, M. Bosch, T.-F. Liu, X. Lian, H.-C. Zhou, *Angew. Chem. Int. Ed.* **2015**, *54*, 14696; *Angew. Chem.* **2015**, *127*, 14909.

Received: May 4, 2016

Published online: ■ ■ ■ ■ ■, ■ ■ ■ ■ ■

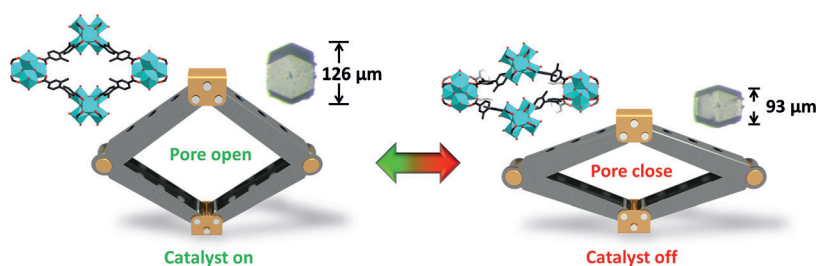
Communications



Metal–Organic Frameworks

S. Yuan, L. Zou, H. Li, Y.-P. Chen, J. Qin,
Q. Zhang, W. Lu,* M. B. Hall,*
H.-C. Zhou* ————— ■■■■-■■■■

Flexible Zirconium Metal-Organic
Frameworks as Bioinspired Switchable
Catalysts



An open and shut case: The inherent cavities and dynamic behavior of flexible MOFs, bear a close resemblance to regulatory enzymes. Switchable activa-

tion and deactivation of their catalytic properties occurs on pore opening and closing by solvation/solvent removal.